2022 International Symposium on Nonlinear Theory and Its Applications,
NOLTA2022, Virtual, December 12-15, 2022

Phonon scattering by discrete breather in nonlinear lattice with potential symmetry

Kazuyuki Yoshimura† and Yudai Hirata‡

†Faculty of Engineering, Tottori University, 4-101 Koyama-Minami, Tottori 680-8552, Japan
‡Department of Engineering, Graduate School of Sustainability Science, Tottori University
4-101 Koyama-Minami, Tottori 680-8552, Japan
Email: kazuyuki@tottori-u.ac.jp

Abstract—We consider the scattering of small amplitude waves (phonons) by a standing discrete breather in two types of one-dimensional nonlinear lattices. Each lattice has a particular symmetry in its equations of motion and is known to exhibit quite anomalous heat transport: one lattice exhibits the ballistic heat transport, i.e., no thermal resistance, and the other an almost ballistic one. We numerically calculate the transmission and reflection rates of phonon wave packets with different wavenumbers. It is shown that almost perfect transmission occurs in one lattice while almost perfect reflection in the other.

1. Introduction

Discrete breather (DB) is spatially localized excitation that can ubiquitously emerge in a variety of nonlinear space-discrete dynamical systems in nature. The concept of DB was introduced by Takeno *et al.* [1, 2]. Mathematically, DBs are time-periodic and spatially localized solutions of the equations of motion in nonlinear lattices. Their existence has been well established by rigorous mathematical analysis [3, 4, 5] and numerical computations [6, 7].

It is known that phonons can be scattered by DBs. The scattering property has been numerically studied in the nonlinear Klein-Gordon lattice [8, 9, 10] and the Fermi-Pasta-Ulam-Tsingou (FPUT) lattice [9]. In weakly nonlinear lattices, thermal energy is transported by phonons. So, it is expected that there is some relation between the scattering property and thermal conductivity of the lattice.

Recently, two types of one-dimensional nonlinear lattices have been constructed, each of which has a particular hidden symmetry. These two lattices are named the *pairwise interaction symmetric lattice* (PISL) [11, 12] and the *umklapp-free lattice* (UFL) [13]. Both lattices are quite anomalous in their heat transport properties: the UFL exhibits the ballistic heat transport, i.e., the heat transport with no thermal resistance, while the PISL exhibits the heat transport close to the ballistic one. This fact suggests that the two lattices show some anomalous properties in the phonon-DB scattering process. In the present paper, we numerically study the scattering of phonons by DBs in the PISl and the UFL.

ORCID iDs Kazuyuki Yoshimura: 0000-0002-4329-4999, Yudai Hirata: 0000-0003-2410-3410

2. Lattice model

Consider a class of one-dimensional nonlinear lattices described by the Hamiltonian

$$H = \sum_{n=-\infty}^{\infty} \frac{1}{2} p_n^2 + \sum_{n=-\infty}^{\infty} \frac{\mu_1}{2} (q_{n+1} - q_n)^2 + \frac{\beta}{4} \sum_{n=-\infty}^{\infty} \sum_{r=1}^{\infty} b_r \left(q_{n+r} - \varepsilon^r q_n\right)^4, \quad (1)$$

where q_n and p_n are the displacement and momentum of nth particle, respectively, $\mu_1 > 0$ is the harmonic coupling coefficient, $\beta > 0$ is the nonlinearity strength, b_r is the coupling strength between the rth neighboring particles, and $\varepsilon \in \{-1, 1\}$. This Hamiltonian describes general nonlinear lattices of unit mass particles which have quartic two-body interactions. Hamiltonian (1) describes the FPUT-β lattice when $b_r = \delta_{r,1}$ and $\varepsilon = 1$, where $\delta_{r,1}$ is Kronecker's delta. The two symmetric lattices, PISL and UFL, are also given by particular cases of Hamiltonian (1): the PISL is the case of $b_r = 1/r^2$ and $\varepsilon = 1$, and the UFL is the case of $b_r = 1/r^2$ and $\varepsilon = -1$.

The equations of motion derived from Hamiltonian (1) are given by

$$\ddot{q}_n = \mu_1 (q_{n+1} - 2q_n + q_{n-1}) + \beta \sum_{r=1}^{\infty} b_r \left[(\varepsilon^r q_{n+r} - q_n)^3 - (q_n - \varepsilon^r q_{n-r})^3 \right], \quad (2)$$

where $n \in \mathbb{Z}$.

3. Symmetry of PISL and UFL

We consider the PISL ($\varepsilon = 1$) and the UFL ($\varepsilon = -1$) in this section. Define the normal mode coordinates $U(k)$ via the discrete Fourier transformation

$$U(k) = \frac{1}{\sqrt{2\pi}} \sum_{n=-\infty}^{\infty} (-\varepsilon)^n q_n e^{-ikn}, \quad (3)$$

where the range of wavenumber is $k \in \mathbb{T} \equiv (-\pi, \pi]$. If we rewrite Eq. (2) in terms of $U(k)$, we can obtain the equation

$$\ddot{U}(k) + \nu_k^2 U(k) = \frac{4\beta}{\pi} \int_{\mathbb{T}^3} dk_1 dk_2 dk_3 \phi_0(k_1, k_2, k_3, k) \times U(k_1)U(k_2)U(k_3)\delta(k_1 + k_2 + k_3 - k), \quad (4)$$

where $U(k)$ depends on time t, ϕ_0 is a time-independent function of (k_1, k_2, k_3, k), δ is Dirac's delta function, and ν_k^2 is the coefficient depending on ε and given by

$$\nu_k^2 = \begin{cases} 4\mu_1 \cos^2(k/2) & \text{if } \varepsilon = 1, \\ 4\mu_1 \sin^2(k/2) & \text{if } \varepsilon = -1. \end{cases} \quad (5)$$

Details of the derivation of Eq. (4) are described in [13].

Ordinary one-dimensional lattices with quartic potentials such as the FPUT-β lattice have the mode couplings specified by both $k_1 + k_2 + k_3 - k = 0$ and $\pm 2\pi$. Equation (4) shows that four normal modes are coupled only when their wavenumbers satisfy the condition $k_1 + k_2 + k_3 - k = 0$ while the couplings of $\pm 2\pi$ are not allowed. This mode coupling rule is a peculiarity of the PISL and the UFL.

The equations of motion of PISL and UFL have a symmetry. In order to describe the symmetry, we introduce the map $\mathcal{S}_\lambda$ defined by

$$\mathcal{S}_\lambda : U(k) \mapsto \begin{cases} U(k) \exp[-ik\lambda] & \text{if } k \in (-\pi, \pi), \\ U(k) & \text{if } k = \pi, \end{cases} \quad (6)$$

where $\lambda \in \mathbb{R}$ is a parameter. It can be shown that Eq. (4) is invariant under the action of $\mathcal{S}_\lambda$ for any $\lambda \in \mathbb{R}$. In this sense, each of the PISL and UFL has a symmetry.

4. Discrete breather and phonon scattering

In Sec. 5, we will consider a finite-size lattice and numerically integrate its equations of motion to investigate the scattering of phonons by a DB placed in the middle of the lattice. For this purpose, we need numerical DB solutions of PISL and UFL. It is possible to numerically compute DB solutions by using the Newton method (cf. [6]) although the existence of DB solutions has not yet been proved for these lattices.

In Fig.1, examples of DB profiles are shown for (a) PISL and (b) UFL, where q_n is shown at the time when the particles have the largest displacements. These examples were calculated by using lattices of size $N = 256$ with periodic boundary conditions. The DBs are time-periodic solutions. For the PISL, they have staggered profiles such that each pair of adjacent particles shows anti-phase oscillation. For the UFL, some center part particles show in-phase oscillation while the other particles in tail parts show anti-phase one. Comparison of the DB profiles for periods $T = 2.0$ and 2.8 indicates that the DB becomes more localized having larger amplitude as the period T decreases or the frequency $\Omega = 2\pi/T$ increases.

We will compare the phonon scattering properties of the PISL and the UFL with that of the FPUT-β lattice in Sec. 5.

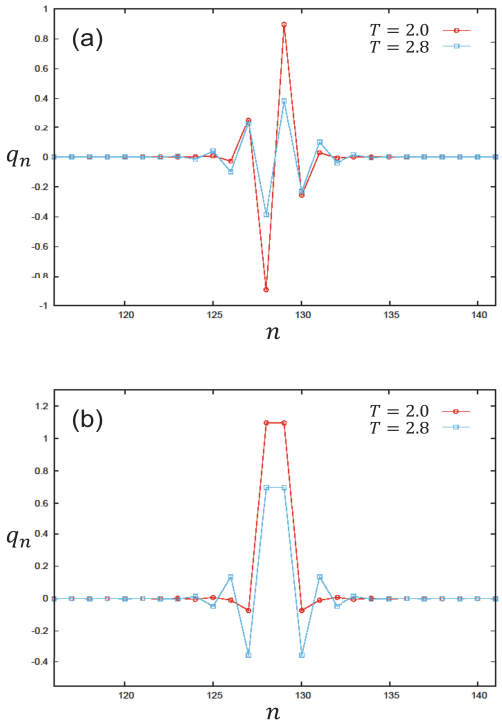

Figure 1: Spatial profile of even symmetric DB for (a) PISL and (b) UFL, Profiles are shown for $T = 2.0$ (red), 2.8 (blue). Parameters are $\mu_1 = 1$ and $\beta = 1$.

It is possible to obtain numerical DB solutions also in the case of the FPUT-β lattice (e.g., see [6, 7]). Moreover, for this lattice, the existence of DBs has been rigorously proved [4, 5].

In our numerical experiments, we use an approximate version of PISL and UFL that has truncated long-range interactions up to length M, which we call the *truncated PISL* and the *truncated UFL*, respectively. The truncated lattices are not exactly symmetric but the asymmetry becomes negligible for large M. The equations of motion of the finite-size truncated PISL or UFL are given as follows:

$$\ddot{q}_n = \mu_1 (q_{n+1} - 2q_n + q_{n-1}) + \beta \sum_{r=1}^{M} b_r \left[(\varepsilon^r q_{n+r} - q_n)^3 - (q_n - \varepsilon^r q_{n-r})^3 \right], \quad (7)$$

where $n = 1, 2, \ldots, N$ and the fixed boundary conditions $q_0 = q_{N+1} = 0$ are assumed. The sum in Eq. (7) is taken only for the terms $(\varepsilon^r q_{n+r} - q_n)^3$ satisfying $n + r \le N$ and the terms $(q_n - \varepsilon^r q_{n-r})^3$ satisfying $n - r \ge 1$.

We describe the procedure of our numerical experiments of phonon scattering by DB. An even DB computed by the Newton method is placed in the middle of the lattice at $t = 0$ as the initial condition. In addition, we place a small-amplitude phonon wave packet propagating to the right at a position $n = n_p$ left of the DB: this wave packet is given

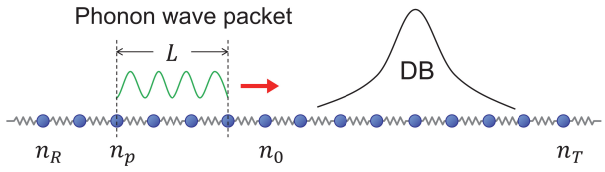

Figure 2: Schematic illustration of phonon scattering numerical experiment.

by $q_n(0) = A(x)\cos kx$ and $p_n(0) = \omega_k A(x)\sin kx$ at $t = 0$, where $k \in (-\pi, \pi]$ is the wavenumber, $\omega_k = 2\sqrt{\mu_1}\sin(k/2)$ is the phonon frequency, $x = n - n_p$, and $A(x)$ is an amplitude envelope such that $0 < A(x) \ll 1$ for $x \in [0, L]$ and otherwise $A(x) = 0$, where L is the wave packet length. The phonon wave packet moves to the right and collides with the DB, and then it is partly transmitted and partly reflected. We measure energy fluxes of the transmitted and reflected waves at two positions $n = n_T$ and n_R, respectively, which are located right and left far away from the DB. Figure 2 shows a schematic illustration of our numerical experiments.

A harmonic approximation is used to measure the energy flux since small-amplitude phonons are assumed. Let $J_T(t)$ be the harmonic energy transported from n_Tth particle to (n_T+1)th one per unit time. This gives the harmonic energy flux of the transmitted phonon, and we have

$$J_T(t) = -\mu_1 \left(q_{n_T+1} - q_{n_T}\right)\left(p_{n_T+1} + p_{n_T}\right)/2. \tag{8}$$

The total energy E_T of the transmitted phonon wave packet is calculated by integrating J_T as follows:

$$E_T = \int_0^\infty J_T(t)\,dt. \tag{9}$$

Similarly, we have $J_R(t) = \mu_1(q_{n_R} - q_{n_R-1})(p_{n_R} + p_{n_R-1})/2$ and the total energy E_R of the reflected phonon wave packet is given by $E_R = \int_0^\infty J_R(t)\,dt$. In addition, we calculate the total energy E_0 of the incident phonon wave packet at a point $n = n_0$. We define the transmission rate r_T and the reflection rate r_R as follows:

$$r_T = \frac{E_T}{E_0}, \quad r_R = \frac{E_R}{E_0}. \tag{10}$$

The relation $r_T + r_R = 1$ holds in good approximation for small-amplitude phonons.

5. Numerical experiments

We carried out numerical experiments for the FPUT-β lattice, the PISL, and the UFL. We compute r_T and r_R as functions of the incident phonon wavenumber k for different values of the DB period T, numerically integrating Eq. (7) by using the Verlet scheme with time step $\Delta t = 0.01$, where the parameters are $\mu_1 = 1$, $\beta = 1$,

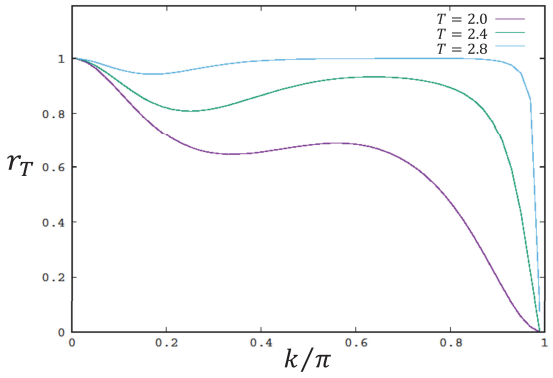

Figure 3: Transmission rate r_T vs phonon wavenumber k for FPUT-β lattice. Results are shown for $T = 2.0$ (purple), 2.4 (green), and 2.8 (blue).

$M = 128$, and $N = 5000$. In each computation, at $t = 0$, an even DB is placed on the lattice so that its center be located between $n = N/2$ and $N/2 + 1$, and an incident phonon wave packet of length $L = 1000$ is placed with its left end at $n_p = 850$. The positions for measuring the transmitted, reflected, and incident energies are set as $n_T = 4250$, $n_R = 750$, and $n_0 = 1900$.

In Fig. 3, the transmission rate r_T of the FPUT-β lattice is plotted against the incident phonon wavenumber k for three different DB periods $T = 2.0$, 2.4, and 2.8. Almost perfect transmission $r_T \simeq 1$ is observed for k close to zero while r_T approaches zero as $k \to \pi$. For intermediate values of k, r_T is significantly smaller than unity, and r_T decreases as T becomes smaller when the value of k is fixed: the DB becomes less transparent.

In Fig. 4, r_T of the PISL is plotted against k. Compared with the FPUT-β lattice, a remarkable feature is that $r_T \simeq 1$ holds for a wide range of k, i.e., the DB is transparent and perfect transmission occurs for most of the wavenumbers. Only for values of k close to π, the transmission rate r_T deviates from unity. It is conjectured that this transparency may be somehow related with high thermal conductivity of the PISL.

In Fig. 5, r_R of the UFL is plotted against k. A remarkable feature here is that $r_R \simeq 1$ holds for a wide range of k, implying $r_T \simeq 0$. That is, the DB is opaque and perfect reflection occurs for most of the wavenumbers. Only for values of k close to π, the reflection rate r_R deviates from unity, implying that those phonons can partly transmit through the DB. This feature is in contrast with that of the PISL and also quite different from the case of FPUT-β lattice. The results in Fig. 5 suggest that phonons would be strongly scattered by DBs if there emerge DBs in thermal conduction states of the UFL, and that the UFL would have a large thermal resistance. On the other hand, the ballistic heat transport has been shown in the UFL [13]. It is con-

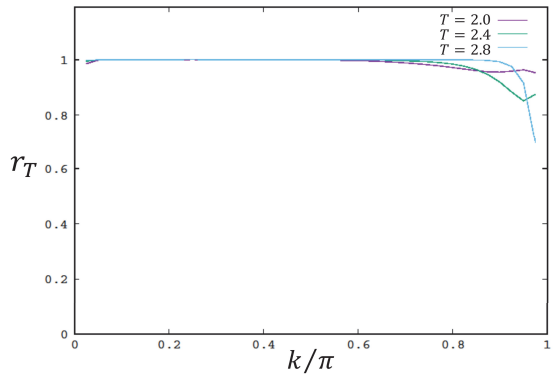

Figure 4: Same as in Fig. 3 but for PISL.

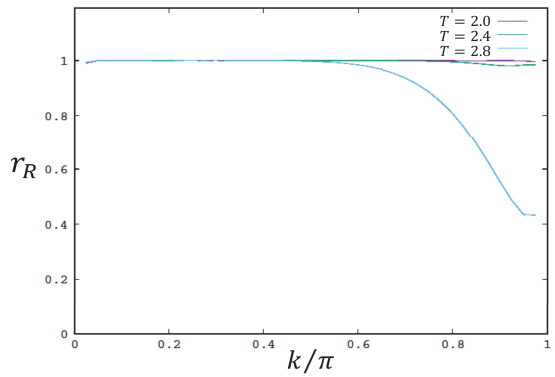

Figure 5: Reflection rate r_R vs phonon wavenumber k for UFL. Results are shown for $T = 2.0$ (purple), 2.4 (green), and 2.8 (blue).

jectured for these two aspects to be compatible that no DB emerges in thermal conduction states of the UFL.

6. Conclusions

We studied the scattering of phonons by a standing DB in the PISL and the UFL, numerically computing the transmission and reflection rates of phonon wave packets. It was found that almost perfect transmission $r_T \simeq 1$ occurs over a wide range of wavenumber k of the incident phonon in the PISL while almost perfect reflection $r_R \simeq 1$ over a wide range of k in the UFL. These behaviors of r_T or r_R are much different from that of the FPUT-β lattice.

Acknowledgments

This work was supported by a Grant-in-Aid for Scientific Research (C), No. 19K03654 from Japan Society for the Promotion of Science (JSPS).

References

[1] S. Takeno, K. Kisoda, and A. J. Sievers, "Intrinsic localized vibrational modes in anharmonic crystals: stationary modes," *Prog. Theor. Phys. Suppl.* vol. 94 pp. 242–269, 1988.

[2] A. J. Sievers and S. Takeno, "Intrinsic localized modes in anharmonic crystals," *Phys. Rev. Lett.*, vol. 61, pp. 970–973, 1988.

[3] R. S. MacKay and S. Aubry, "Proof of existence of breathers for time-reversible or Hamiltonian networks of weakly coupled oscillators," *Nonlinearity*, vol. 7, pp. 1623–1643, 1994.

[4] G. James, "Centre Manifold reduction for quasilinear discrete systems," *Jour. Nonlinear Sci.*, vol. 13 pp. 27–63, 2003.

[5] K. Yoshimura and Y. Doi, "Existence of odd, even, and multi-pulse discrete breathers in infinite Fermi-Pasta-Ulam lattices," *Jour. Diff. Eq.*, vol. 298, pp. 560–608, 2021.

[6] J. L. Marin, S. Aubry, "Breathers in nonlinear lattices: numerical calculation from the anticontinuous limit," *Nonlinearity*, vol. 9, pp. 1501–1528, 1996.

[7] B. Sánchez-Rey, G. James, J. Cuevas, and J. F. R. Archilla, "Bright and dark breathers in Fermi-Pasta-Ulam lattices," *Phys. Rev. B*, vol. 70, 014301, 2004.

[8] T. Cretegny, S. Aubry, and S. Flach, "1D phonon scattering by discrete breathers," *Physica D*, vol. 199, pp. 73–87, 1998.

[9] S. Flach, A. E Miroshnichenko, and M. V. Fistula, "Wave scattering by discrete breathers," *Chaos*, vol. 13, pp. 596-609, 2003.

[10] F. Hadipour, D. Saadatmand, M. Ashhadi, A. Moradi Marjaneh, I .Evazzade, A. Askari, S. V. Dmitriev, "Interaction of phonons with discrete breathers in one-dimensional chain with tunable type of anharmonicity," *Phys. Lett. A*, vol. 384, 126100, 2020.

[11] Y. Doi and K. Yoshimura, "Symmetric Potential Lattice and Smooth Propagation," *Phys. Rev. Lett.*, vol.117, 014101, 2016.

[12] Y. Doi and K. Yoshimura, "Construction of nonlinear lattice with potential symmetry for smooth propagation of discrete breather," *Nonlinearity*, vol.33, pp.5142–5175, 2020.

[13] K. Yoshimura and Y. Doi, "Heat transport in nonlinear lattices free from the Umklapp process," *Phys. Rev. E*, vol.105, 024140, 2022.